coatings

MDPI

Article

Study on Improving Electrochemical Machining Performances through Energy Conversion of Electrolyte Fluid

Zhenghui Ge, Maolong Chen, Wangwang Chen and Yongwei Zhu *

College of Mechanical Engineering, Yangzhou University, Yangzhou 225127, China; zhge@yzu.edu.cn (Z.G.); mlchen319@163.com (M.C.); wwchen319@163.com (W.C.)
* Correspondence: ywzhu@yzu.edu.cn

Abstract: Electrochemical machining (ECM) is regarded as a promising and cost-effective manufacturing method for difficult-to-cut materials with complex shapes and structures. The flow-field state of machining gaps is considered a key factor affecting machining performance in ECM engineering practice and has been widely studied. However, little attention has been given to the fluid energy of electrolytes during the ECM process. This study mainly focuses on the influence of the conversion between dynamic and static pressure energy of electrolyte fluid on ECM performance. The simulation results show that by changing the degree of convergence of the electrolyte outlet, the dynamic and static pressure energy of the electrolyte can be effectively adjusted, and increased static pressure energy can be obtained by sacrificing dynamic pressure energy. The experimental results show that electrolyte energy conversion can achieve better surface quality and material removal rate (MRR). However, excessive sacrifice of fluid dynamic pressure energy will also worsen the ECM performance. By combining MRR and Ra, moderate fluid energy conversion can achieve better machining performance, with a degree of convergence of around 50%–70%. The experimental results also show that moderate energy conversion of the electrolyte fluid can improve the utilization efficiency of electrical energy in the ECM process. This may be because the static pressure of the electrolyte can effectively compress the volume of gas products and reduce the electrical resistivity of the machining gap. These conclusions can provide some useful assistance for ECM engineering practice.

Keywords: electrochemical machining; flow field; fluid energy conversion; machining performance; numerical simulation

check for updates

Citation: Ge, Z.; Chen, M.; Chen, W.; Zhu, Y. Study on Improving Electrochemical Machining Performances through Energy Conversion of Electrolyte Fluid. *Coatings* **2024**, *14*, 406. https://doi.org/10.3390/coatings14040406

Academic Editor: Peter Rodič

Received: 29 February 2024
Revised: 18 March 2024
Accepted: 26 March 2024
Published: 29 March 2024

Copyright: © 2024 by the authors. Licensee MDPI, Basel, Switzerland. This article is an open access article distributed under the terms and conditions of the Creative Commons Attribution (CC BY) license (https://creativecommons.org/licenses/by/4.0/).

1. Introduction

Electrochemical machining (ECM) is a non-traditional machining technology that removes material in the form of ions based on electrochemical anodic dissolution. Compared with traditional machining methods, ECM has significant technical advantages, such as a high material removal rate, good surface quality, no tool wear, etc. [1,2]. ECM is considered a promising and cost-effective manufacturing method for the fabrication of difficult-to-cut materials with complicated shapes and structures and is widely used in aerospace, weapons, energy, medical, bioengineering, and other industrial fields [3–6].

In the ECM process, there is no contact between the anode workpiece and the cathode tool, and the electrolyte flows through the machining gap at a high velocity of about 10–30 m/s to remove machined products, such as metallic hydroxides, gases, joule heat, etc. [7,8]. The flow-field parameters of the machining gap have a key influence on the morphology and distribution of machined products, which have important impacts on the machining performance of ECM [9,10]. Therefore, both academia and industry attach great importance to the study of the flow field in the ECM process.

The flow-field mode is regarded as a key factor in ensuring machining stability, machining accuracy, and surface quality. Selecting the appropriate flow-field mode for different machining objects is the basis of successful ECM, and many scholars have conducted much

research on this. Xu et al. analyzed the advantages and disadvantages of the forward flow mode, lateral flow mode, and reverse flow mode separately and designed a π-type flow-field mode for the electrochemical machining of a blisk cascade passage, which increased the cathode feed rate by 70% [11,12]. Zhu et al. designed a dual-channel flow mode for the machining of blades, which improved the uniformity of the flow field around the blade and effectively increased the cathode feed rate and surface quality [13,14]. Wang et al. designed tangential flow based on the structural characteristics of a large-sized blade, which effectively eliminated defects caused by sudden changes in the flow channel and improved the uniformity of the electrolyte flowing into the concave and convex surfaces of the blade [15]. Li et al. proposed a snake-shaped channel mode for through-mask ECM of large-area hole array structures, which effectively improved the dimensional consistency of hole group structure [16]. Liu et al. further proposed the "coded flow field" mode based on a serpentine channel, which shortens the electrolyte flow path by alternately arranging the inlet and outlet on the cathode, further improving the surface quality [17]. Tang et al. compared the influence of different flow modes on ECM of a closed integer impeller. The results showed that the reverse flow mode achieved a higher electrolyte velocity and better machining results than the forward flow mode [18].

The structure of the cathode tool also has an important influence on the flow field in the machining gap, which has been widely studied by many scholars. Liu et al. designed three circular, rectangular, and triangular internal jet electrodes. The results showed that an electrode tool with a triangular internal flow channel can significantly reduce stray corrosion and surface roughness [19]. Yang et al. improved the uniformity of the flow field and addressed the insufficient liquid supply by optimizing the cathode structure and realized the high-quality machining of a deep spiral hole with a gradually changing groove section [20]. Ge et al. designed various internal spray electrode structures and achieved efficient and large allowance removal of casing parts by optimizing the internal spray electrode [21]. Zou et al. designed a rotary wire electrode with a cutting edge for cutting experiments, and the results showed that a shaped electrode tool can improve the renewal rate of the electrolyte and accelerate the elimination of machined products [22]. Zou et al. established an electrochemical drilling flow-field model and simulated the axial flow-field distribution of the nozzle. The optimized nozzle structure was obtained through the golden ratio method, the deviation was successfully processed within ±0.04 mm, and the inner surface roughness was less than Ra = 0.5 μm [22]. Jia et al. designed a cathode structure with four incremental baths, effectively improving the uniformity and bubble content of the electrolyte in the machining gap. A qualified sample was machined using the optimized process parameters with a deviation of 0.28 mm and a roughness of 1.398 μm [23]. Tang et al. carried out cathode optimization for ECM of an internal spiral. The results showed that a uniform flow field was obtained at a supply angle of 40°, and an inner spiral specimen with a length of 800 mm was successfully machined [24].

Optimizing the fluid parameters is also regarded as an important method to improve the flow-field characteristics and machining performance. Chai et al. analyzed the influence of electrolyte inlet pressure on the side gap of a gas film hole. The results showed that too high or too low electrolyte pressure is not conducive to ensuring machining accuracy, and a smaller error can be obtained with an optimized inlet pressure of 0.6 MPa [25]. Shin et al. studied the effect of electrolyte concentration on machining performance. The results showed that increasing the electrolyte concentration can effectively improve the cathode feed rate, but it will also lead to a decrease in the forming accuracy of the microstructure [26]. Fang et al. introduced pulsating electrolyte flow to the ECM process and effectively enhanced the transfer ability of heat and mass of the electrolyte in the machining gap [27]. Qu et al. proposed the use of progressive electrolyte pressure during ECM of blisk channels, which effectively improved the cathode feed rate [28]. Hu et al. proposed the application of compressed air to form a gas film around the workpiece surface, so as to promptly remove stray corrosion from the non-machined area [29]. Hewidy et al. effectively suppressed the interruption of electrolyte flow by adding orbital electrode movement and improved

the machining stability [30]. Zhao et al. obtained optimized experimental parameters through simulation and improved the machining quality and stability of the ECM of a slot workpiece [31]. Cao et al. proposed a strategy of periodically changing the direction of electrolyte flow in counter-rotating electrochemical machining [32]. The experimental results verified the effectiveness of the periodic flow field, and the authors successfully processed a convex structure with a deviation of <0.05 mm.

The above studies fully showed that the flow field is the key factor for high-quality ECM, and research on flow-field characteristics has important guiding significance for the engineering application of ECM technology. Recently, many studies have shown that changing the outlet state of the flow field also has an important impact on the flow-field state in the machining gap. For example, in the ECM process of blades, Xu et al. found that by optimizing the outlet-cornered gap, the flow-field parameters in the machining gap could be optimized, which effectively promoted the stability and efficiency of the machining [33]. Furthermore, Ge et al. improved the flow-field state by increasing the electrolyte outlet back pressure in the ECM process of casings, and the forming height of convex structures on casing surfaces was significantly improved [34]. However, there are few reports on the specific influence mechanism and law of this method in the ECM process. In this paper, a variable cross-section ECM fixture device was carefully designed to adjust the dynamic and static pressure energy of the electrolyte fluid in the machining gap, and a series of simulations and experiments was carried out. A detailed discussion was conducted on the conversion relationship of dynamic and static pressure parameters in the electrolyte channel under different degrees of convergence, as well as their impact on ECM performance.

2. Methodology

ECM is a complex material removal process driven by the multi-physical-field synergy of the electric field, flow field, temperature field, etc. During the ECM process, the anode and cathode undergo different electrochemical reactions. The main reactions that occur at the cathode are as follows:

$$2H_2O + 2e^- \rightarrow H_2 + 2OH^- \quad (1)$$

The main reactions that occur at the anode are as follows:

$$M^0 \rightarrow M^{n+} + ne^- \quad (2)$$

where M^{n+} represents metal ions.

Due to the voltage difference applied between the anode workpiece and the cathode tool, the surface material of the workpiece gradually dissolves, and the machining gap is filled with machining products (such as metal precipitates, bubbles, heat, etc.) during the ECM process [35,36]. Generally, high-speed flowing of the electrolyte is regarded as an important way to eliminate machining products in time and improve machining performance. However, many studies have also shown that blindly increasing the electrolyte velocity cannot have a significant impact on the machining performance because ECM is a complex multi-physics coupling process [37,38]. This study proposes an interesting approach to improve machining performance through energy conversion of electrolyte fluid during ECM processes, as shown in Figure 1. While keeping other machining conditions unchanged, the dynamic and static pressure energies of the electrolyte fluid in the machining gap are optimized by simple external means to achieve the effect of improving machining performance.

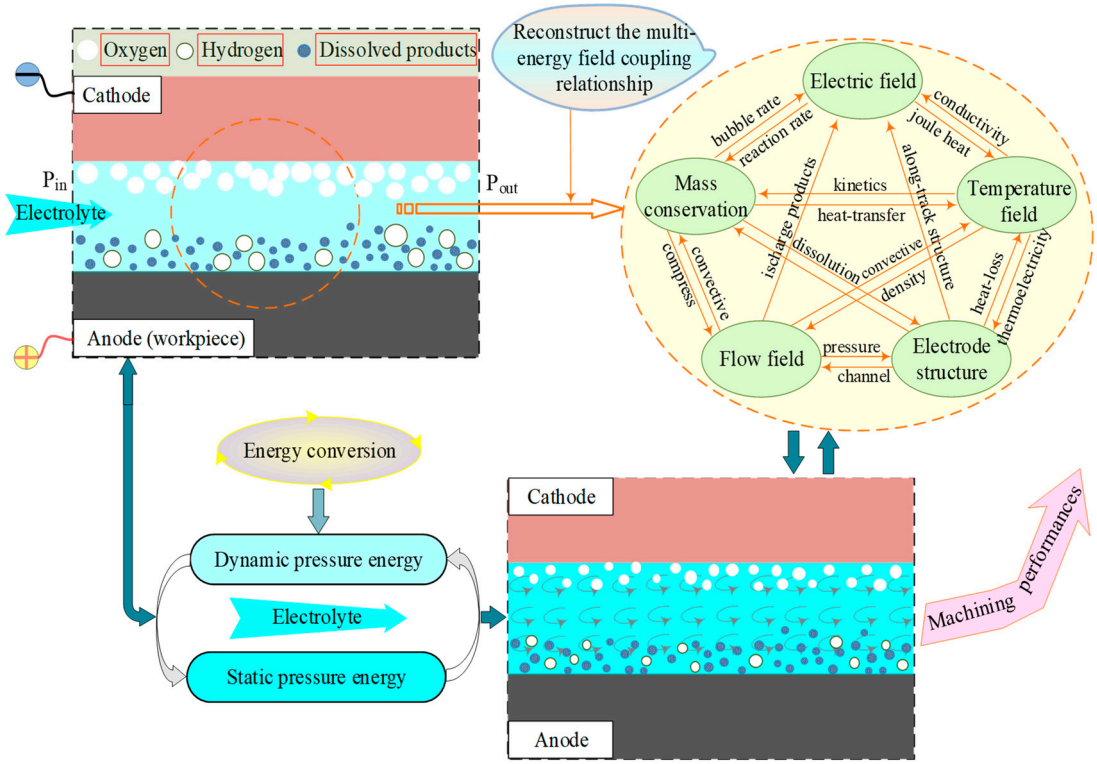


Figure 1. Schematic diagram of the proposed method of optimizing machining performance.

Based on the ideal fluid assumption, ignoring energy loss along the electrolyte channel, the fluid energy at the inlet and outlet follows the principle of mechanical energy conservation as follows:

$$p_{in} + \frac{1}{2}\rho v_{in}^2 + \rho g h_{in} = p_{out} + \frac{1}{2}\rho v_{out}^2 + \rho g h_{out} \tag{3}$$

where p_{in} and p_{out} are the static pressure energy at the inlet and outlet of the fluid, respectively; v_{in} and v_{out} are the fluid velocity at the inlet and outlet, respectively; p is fluid density; g is the acceleration of gravity; and h_{in} and h_{out} are the heights of the fluid at the inlet and outlet, respectively.

In the ECM system, the potential energy can usually be ignored, so reducing the dynamic pressure energy can obtain correspondingly increased static pressure energy. According to the conversion relationship between the dynamic pressure energy and the static pressure energy expressed in Equation (3), it can be seen that higher static pressure energy can be obtained by sacrificing electrolyte flow velocity because the static pressure energy is the square of the electrolyte flow velocity.

Owing to the conversion of the fluid energy, the electrolyte fluid will form a stronger compression effect on the bubbles contained in the machining gap according to the ideal gas equation, as shown in Equation (4), having an important impact on electrolyte conductivity according to Equation (5).

$$pV = nRT \tag{4}$$

where p is the electrolyte pressure, R is the ideal gas constant, and T is the gas temperature.

$$\kappa = \kappa_0[1 + \xi(T - T_0)](1 - \beta_g)^n \tag{5}$$

where ξ is the temperature coefficient determined by the electrolyte, n is the bubble influence coefficient, κ_0 is the conductivity of the electrolyte at the inlet, and T_0 is the electrolyte temperature at the inlet.

With the help of the synergetic coupling relationship of the multi-physical field during the ECM process, the method of optimizing fluid energy conversion proposed in this paper interacts with the electric field, temperature field, mass transfer process, etc., which may have many positive impacts on the machining performance in the ECM process according to Equation (6).

$$m = \eta\omega\rho_{\mathrm{m}} \int \frac{U \cdot A \cdot \kappa_0[1 + \xi(T(t) - T_0)]\left[1 - \beta_{\mathrm{g}}(t)\right]^n}{\Delta(t)} tdt \tag{6}$$

where A is the machining area, t is the machining time, I_{t} is the machining current that can be collected during the ECM process, $\Delta(t)$ is the machining gap between the cathode and anode in the electrolyte channel with different times, η is the current efficiency, ω is the volume electrochemical equivalent, ρ_{m} is the anode material density, and U is the voltage difference between the anode and cathode.

3. Experiment Preparation

The experimental set-up consists of a tool motion control system, electrolyte circulation system, power supply system, and current detection system, as shown in Figure 2. In order to better realize the principle and method proposed in this study, the fixture applied in this study was carefully designed, and its outlet section can be adjusted through the section-regulating valve at the tail. This design is very easy to implement and use in engineering practice. To better compare the experimental results under different degrees of convergence, the machining time was set to 3 min, and other parameters were kept constant, as shown in Table 1. Additionally, in order to better study the influence of the proposed method on dynamic pressure energy and static pressure energy of electrolyte fluid in the machining gap, a series of simulation experiments was conducted using commercial simulation software in this study. The inlet pressure was uniformly set to 0.04 MPa, and the outlet pressure was uniformly set to 0 MPa. The degree of convergence of the electrolyte outlet section was controlled at 0% (normal outlet without contraction), 12%, 34%, 56%, and 78%. The degree of convergence is described as Equation (7).

$$C = \frac{A_{\mathrm{n}}}{A_0} \tag{7}$$

where C is the degree of convergence, A_0 is the initial outlet area, and A_{n} is the outlet area after convergence.

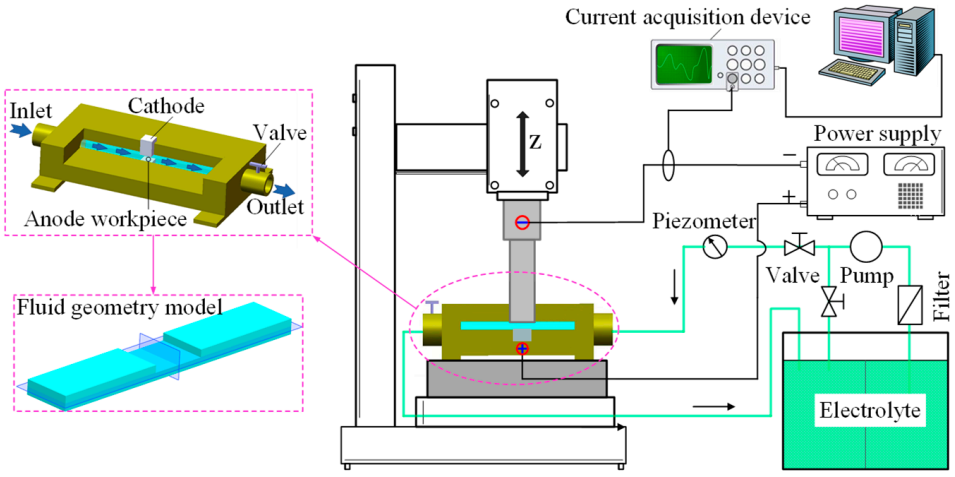


Figure 2. Schematic diagram of experimental set-up.

Table 1. Experimental conditions.

Parameter	Value
Workpiece material	Stainless steel
Cathode material	Stainless steel
Electrolyte inlet pressure (MPa)	0.04 MPa
Degree of convergence	From 0% to 78%
Electrolyte	10% $NaNO_3$
Electrolyte temperature (°C)	25

In this study, the workpiece material was 304SS alloy; its main metal composition is shown in Table 2. Specimens in the form of cubes were specially prepared, and all specimens were cleaned by ultrasonically to remove surface oil stains and impurities before and after the ECM experiment. The surface roughness, microstructure, and composition of the specimens machined under different conditions were investigated using a surface-finish instrument (Perthometer S3P, Mahr GmbH, Göttingen, Germany) and a field emission scanning electron microscope (GeminiSEM 300, Carl Zeiss, Jena, Germany). The machined specimens were cleaned and weighed carefully before and after the experiment to evaluate the material removal rates (MRRs) of anode workpieces under different conditions. The MRR is calculated using the following equation:

$$\mathrm{MRR} = \frac{m}{t} \tag{8}$$

where m is the total removal of material mass during the machining time (t).

Table 2. Main metal composition of 304SS (wt %).

Fe	Ni	Cr	C	Si	Mn
Balance	8.92	18.38	0.08	1.00	2.00

4. Results and Discussions

4.1. Regulation of Dynamic Pressure and Static Pressure in the Electrolyte Channel

In order to better verify and visually express the impact of outlet section changes on the conversion of dynamic pressure and static pressure in the electrolyte channel, we conducted a series of simulation experiments under different conditions. Figure 3 shows the variation of static pressure energy and dynamic pressure energy of electrolyte fluid under different degrees of convergence 0%, 34%, and 78%. It can be seen that the degree of convergence of the outlet can effectively change the static pressure energy of the electrolyte fluid in the channel, and with an increase in the degree of convergence, the static pressure energy of the electrolyte fluid also increases sharply, as shown in Figure 3a–c. On the other hand, unlike the variation of static pressure energy, the electrolyte velocity in the channel decreases with an increase in the degree of convergence, which means that the dynamic pressure energy of the electrolyte decreases with an increase in the degree of convergence, as shown in Figure 3d–f. These phenomena are consistent with the principle of Equation (3), which shows that it is feasible to regulate the dynamic pressure energy and the static pressure energy of the electrolyte fluid by adjusting the outlet area.

To determine the influence of the degree of convergence on fluid energy conversion in the electrolyte channel, in this section, we further quantitatively analyze the fluid performance in the electrolyte channel under different degrees of convergence. It can be clearly seen that the variation of static pressure energy of the electrolyte fluid is not linearly related to the change of the degree of convergence. In the initial stage, the degree of convergence of the outlet has little effect on the static pressure energy of the electrolyte fluid, but when the degree of convergence of the outlet exceeds 34%, the static pressure energy of the electrolyte fluid increases sharply with the degree of convergence. In particular, when the degree of convergence increased to 78%, the static pressure of the electrolyte

fluid rose to several times that at 0%, as show in Figure 4a. This means that sufficient static pressure energy can be obtained by using an appropriate degree of convergence, thus effectively compressing the bubbles in the electrolyte fluid to achieve a positive effect in terms of improving electrolyte conductivity. Furthermore, it is noteworthy that although the electrolyte fluid velocity decreases with the increase in degree of convergence, the decrease is not obvious, which is significantly different from the variation rule for static pressure energy with the degree of convergence, as show in Figure 4b. For example, compared with a 0% degree of convergence, when the degree of convergence is 56%, the electrolyte fluid velocity decreases by less than 20%, while the electrolyte static pressure increases by more than twice. These phenomena are perfectly consistent with the principles and expectations described in Section 2.

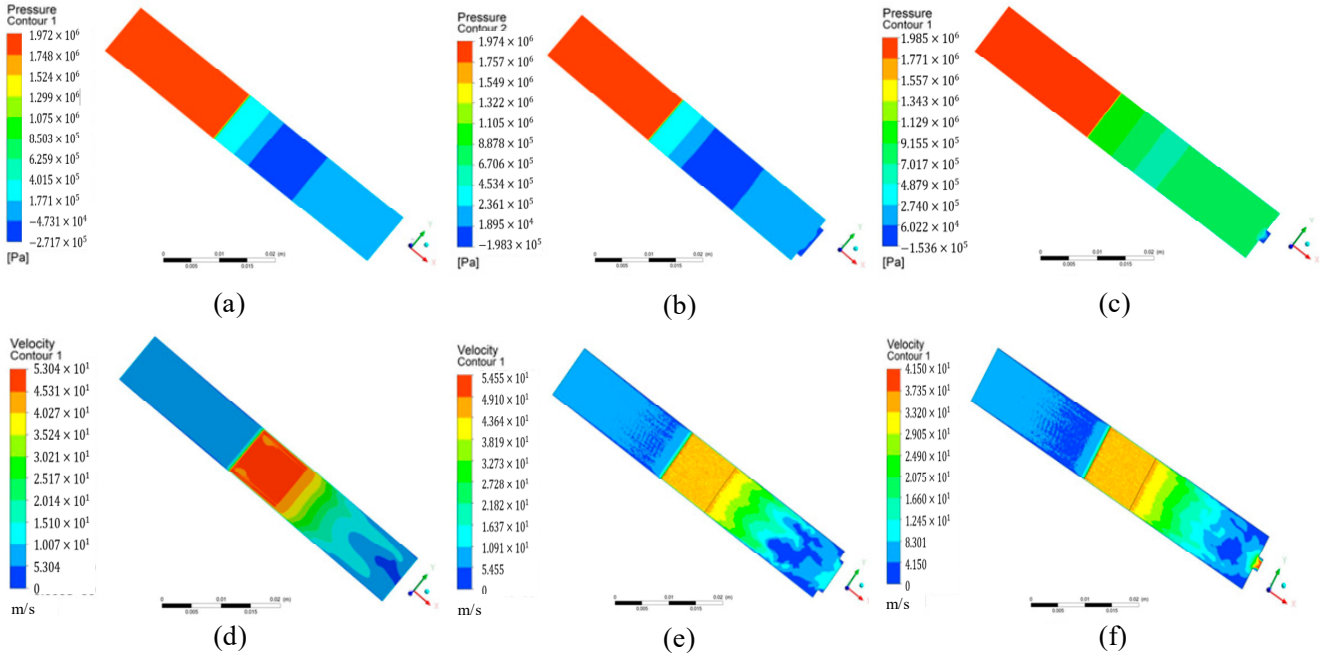


Figure 3. Pressure contour and velocity contour of electrolyte channel under different degrees of convergence: (**a**) and (**d**) 0%; (**b**) and (**e**) 34%; (**c**) and (**f**) 78%.

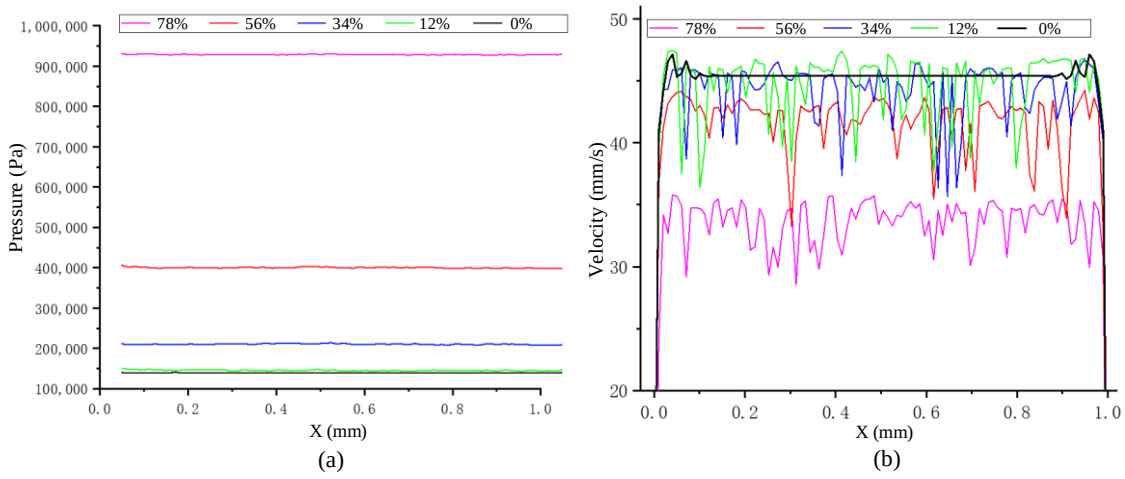


Figure 4. Pressure distribution and velocity distribution of electrolyte under different degrees of convergence: (**a**) pressure; (**b**) velocity.

4.2. Effect of Fluid Energy Conversion on Surface Morphology of ECM

To further explore the influence of fluid energy conversion on ECM performance, we conducted a series of experiments with different degrees of convergence, as changes can cause fluid energy conversion in the electrolyte channel. From Figure 5a, it can be seen that the surface of the machined specimen is rough under the normal outlet mode, and more machined products remain. With the increase in the degree of convergence, the amount of machined products gradually decreased, and the surface of the machined specimens also became gradually brighter, as shown in Figure 5b–e. This indicates that adjusting the fluid dynamic pressure and static pressure energy by increasing the degree of convergence of the electrolyte outlet is beneficial in terms of promoting the removal of machined products. As the degree of convergence further increased to 75%, uneven corrosion occurred on the specimen surface, as shown in Figure 5f. This indicates that excessive fluid energy conversion as a result of increasing the degree of convergence of the electrolyte outlet can have a negative impact on ECM performance.

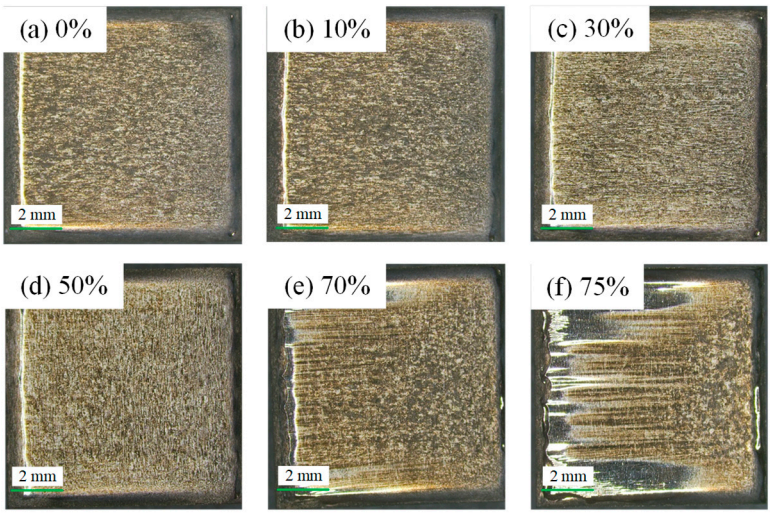


Figure 5. Specimens machined by ECM under different degrees of convergence.

Figure 6 shows the micro-morphology of machined specimens under different degrees of convergence. It can be seen that when the normal outlet mode is adopted, a large number of machining products are attached to the surface of the machined specimen, as shown in Figure 6a. With the gradual increase in the degree of convergence, the products attached to the machined surface are gradually broken and fall off. When the degree of convergence rises to about 30%, the products attached to the specimen surface fall off in a large area, but there are still many products remaining on the surface of the machined specimen. This may be considered as the main reason for the unevenness of the machined surface when the degree of convergence is small, as shown in Figure 6b,c. With the further increase in the degree of convergence, the amount of products remaining on the machined surface gradually decreases, and the machined surface becomes progressively more smooth, as shown in Figure 6d,e. When the degree of convergence reaches 75% or more, uneven corrosion occurs on the machining surface, leading to severe damage to the surface morphology of the machined specimens, and a large number of ripples are generated on the machining surface, as shown in Figure 6f. This may be due to the significant decrease in the dynamic pressure energy of the electrolyte fluid under a 75% degree of convergence, resulting in a sharp decrease in fluid velocity within the machining gap, which cannot meet the requirements of the ECM process for electrolyte velocity.

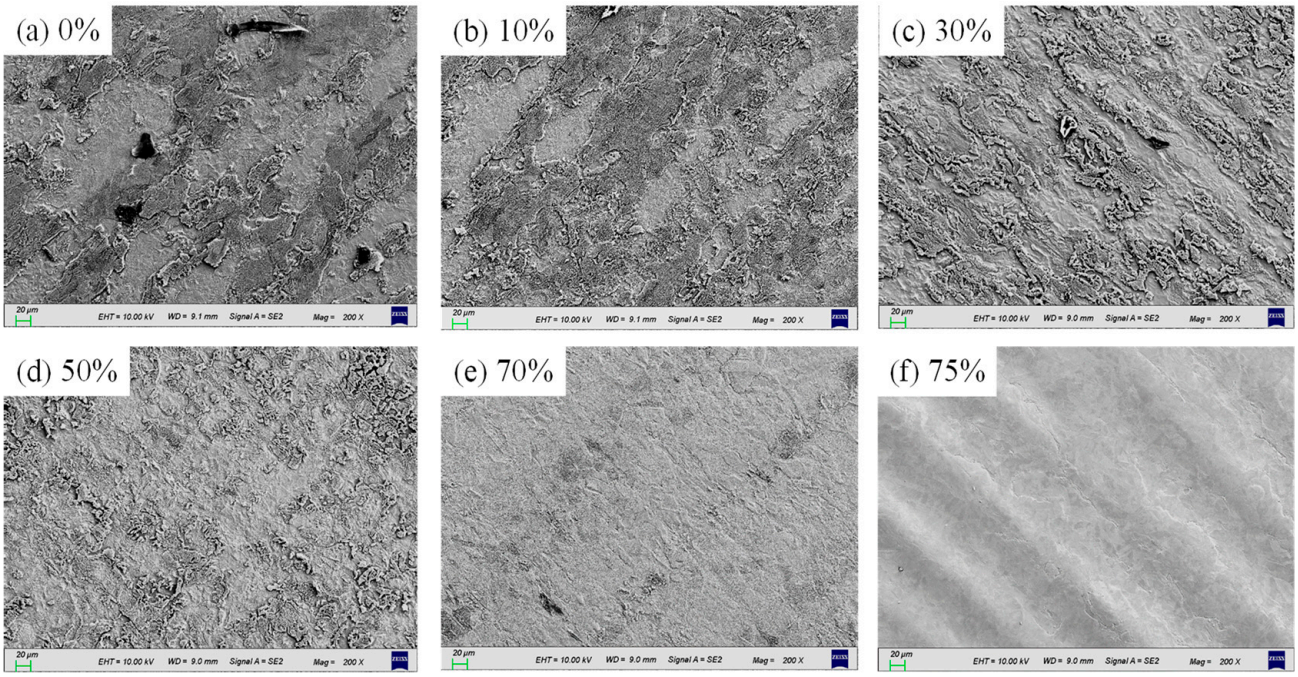


Figure 6. Micro-morphology of specimens machined by ECM under different degrees of convergence.

4.3. Effect of Fluid Energy Conversion on MRR of ECM

Figure 7 shows the MRRs and surface roughness of the machined specimens under different degrees of convergence. It can be seen that the MRR gradually improves with the increase in the degree of convergence and reaches a peak of 0.292 g/min with a degree of convergence of about 50%. After the degree of convergence is greater than 75%, the MRR shows a cliff-like decline. On the other hand, the variation of surface roughness of machined specimens is relatively complex with the increase in the degree of convergence. It can be seen that in the initial stage, the surface roughness of machined specimens increased from 0.402 μm to 0.641 μm. Subsequently, the surface roughness of the machined specimens gradually decreased with the increase in the degree of convergence and reached the lowest reading of 0.345 μm at a 70% degree of convergence 70%. After that, the surface roughness of machined specimen increased sharply with the further increase in the degree of convergence due to the seriously uneven corrosion on the machined part, as shown in Figure 5f. Based on the comprehensive effect of MRRs and surface roughness, a degree of convergence between 50% and 70% may be regarded as the optimal range. This indicates that increasing the static pressure energy of the electrolyte fluid has a significant positive impact on ECM performance but that excessive static pressure energy can also have a serious negative impact on ECM performance due to insufficient dynamic pressure energy of the electrolyte fluid. Therefore, in order to achieve high-performance ECM, the appropriate degree of convergence of the electrolyte outlet should be carefully selected to optimize the dynamic pressure energy and static pressure energy of the electrolyte fluid in the machining gap.

Figure 7 also shows the change of fluid velocity in the machining gap under different degrees of convergence, which is calculated according to Equation (6). It can be seen that the fluid velocity in the machining gap decreases slowly with the increase in the degree of convergence. When the degree of convergence reaches about 50%, the fluid velocity in the machining gap still remains above 10 m/s, which fully meets the electrolyte velocity requirements of the ECM process [26,29]. This indicates that although increasing the static pressure energy of the electrolyte fluid will lead to a decrease in the dynamic pressure energy of the electrolyte fluid, it will have a minimally negative impact on the ECM process due to the small change in fluid velocity.

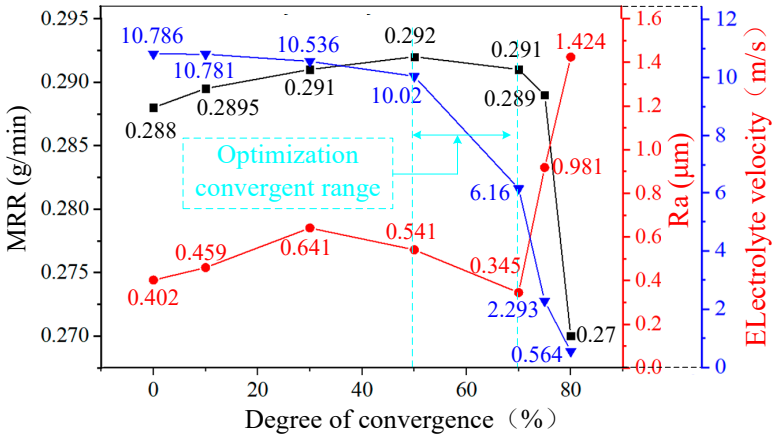


Figure 7. MRR, surface roughness, and electrolyte velocity under different degrees of convergence.

It is worth noting that when the degree of convergence is greater than 50%, the electrolyte velocity begins to sharply decrease. When the degree of convergence reaches about 70%, the fluid velocity of the machining gap drops to 6.16 m/s, but the MRR is still higher than the normal outlet mode, which further proves that better machining performance can be achieved through appropriate energy conversion of electrolyte fluid during ECM processes. After that, as the degree of convergence continues to increase to about 75%, the fluid velocity of the machining drops sharply to less than 2.293 m/s, which is significantly lower than that required by ECM, thereupon then resulting in a cliff-like drop in the MRR.

$$v = \frac{Q}{lb} \tag{9}$$

where Q is the flow in units of time, and l and b are the lengths of lines 1 and 2, respectively.

4.4. Effect of Fluid Energy Conversion on Machining Performance under Different Current Densities

In the engineering practice of ECM, current parameters usually have a large range of variation. Therefore, we conducted further experimental research on the effect of fluid energy conversion on ECM performance under different current densities. Based on the results discussed in Sections 4.2 and 4.3, a degree of convergence of 50% was selected for the experimental work described in this section. Throughout the entire experiment, the current parameters were kept constant. Figure 8 shows the micro-morphology of machined specimens with a 50% degree of convergence. It can be seen that under the condition of low current density (5 A/cm^2 and 10 A/cm^2), the micro-morphology of the machined specimen is very rough, which is caused by the selective corrosion of different elements. With the increase in current density, the passivation layer becomes loose, and the machined products fall off and are flushed away from the machining gap by the electrolyte more easily so that the surface quality of the machined specimen is gradually improved (15 A/cm^2 and 20 A/cm^2). This process is basically consistent with the law of the normal ECM process.

Figure 9 shows the changes of voltage parameters during the machining process with different current densities under the conditions of a normal outlet mode and a convergent flow mode. It can be seen that the voltage increment of the convergent flow mode is smaller than that of the normal outlet mode. This is because the current efficiency under sodium nitrate solution conditions is less than 100%, as shown by the blue line in Figure 9, which can be calculated by Equation (10). That is to say, in addition to the hydrogen released from the cathode during ECM processes, the anode will also release oxygen, resulting in a large amount of gas in the machining gap.

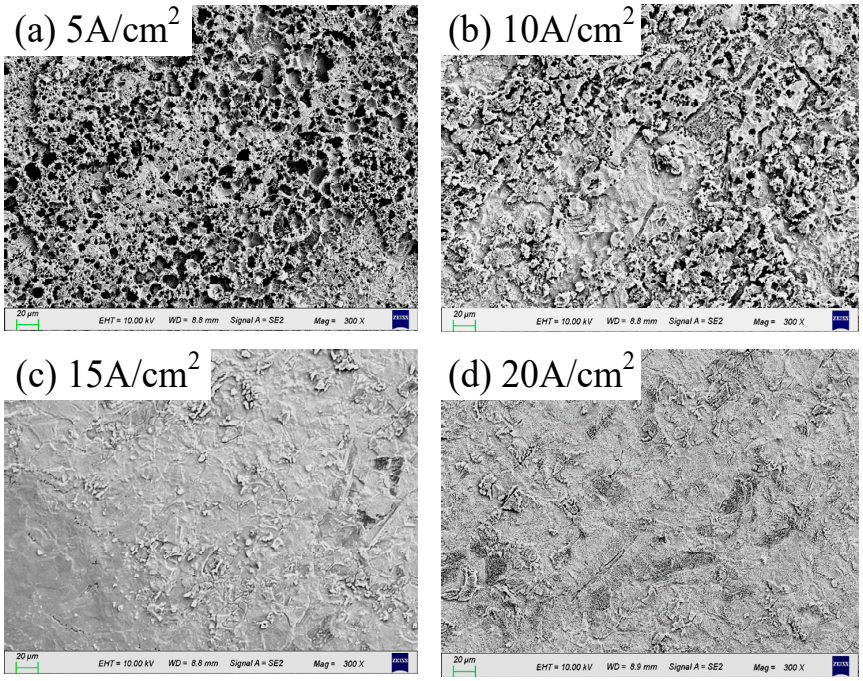


Figure 8. Micro-morphology of specimens machined by ECM at different current densities.

$$\eta = \frac{\Delta m_{\exp}}{It}\left(F\left(\frac{n_1}{A_1}a_1 + \frac{n_2}{A_2}a_2 + \ldots + \frac{n_q}{A_q}a_q\right)\right) \tag{10}$$

where $\Delta m_{\exp}$ is the actual dissolution mass (g), I is the current (A), t is the machining time in each run (s), F is the Faraday constant, q represents the element number, a represents the percentage of each element, n is the valence of the dissolved element, A is the relative atomic mass of the element, and a the material composition proportion of the machining object, as shown in Table 1.

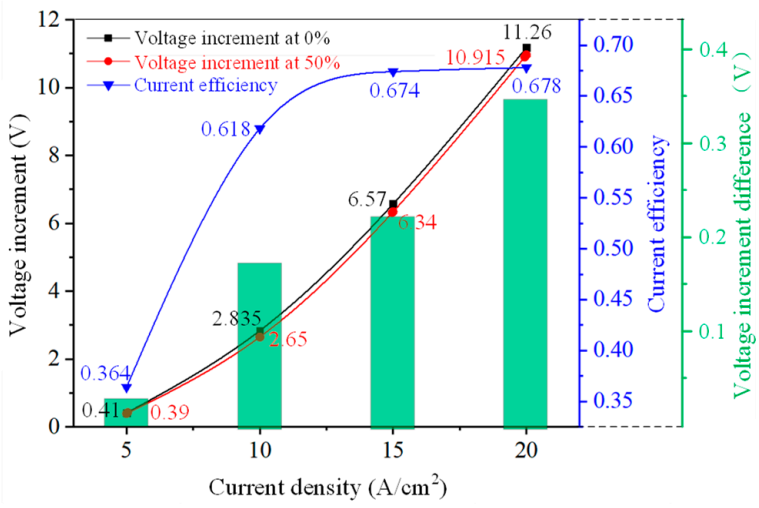


Figure 9. Variation of voltage parameters and current efficiency under different current densities.

It is worth noting that gas is easy to compress according to Equation (4). Combined with the simulation results reported in Section 4.1, the pressure in the machining gap under the convergent flow mode is significantly higher than that under the normal outlet mode. This indicates that the bubble volume in the machining gap under the convergent flow mode is lower than that under the normal outlet mode. As we know, the gas volume content in the machining gap is closely related to the electrolyte conductivity (Equation (5)),

so the electrolyte conductivity in the machining gap under the condition of the convergent flow mode is higher than that in the normal outlet mode, which can be regarded as the main reason why the voltage increment of the convergent flow mode is smaller than that of the normal outlet mode in this paper, as shown by the red dotted line and black square dotted line in Figure 9.

Furthermore, under the condition of constant-current ECM, the electric energy consumed during machining can be described by Equation (11). It can be seen that under the same conditions, the electric energy consumed by the convergent flow mode is lower than that consumed by the normal outlet mode due to the difference in voltage increment. This indicates that in the ECM process, the conversion of electrolyte fluid energy can not only achieve better machining performance but also save electric energy, which is conducive to the realization of low-carbon manufacturing.

$$W = \int_0^t \frac{(U_0 + U_t)I}{t} t dt \tag{11}$$

where U_0 is the initial voltage, U_t is the voltage increment with respect to time, and I is the machining current.

5. Conclusions

This study mainly focuses on the influence mechanism and law of the conversion between dynamic and static pressure energy of electrolyte fluid with respect to ECM performance. A number of simulations and experiments were carried out, and machined specimens were examined, calculated, and analyzed. The conclusions can be summarized as follows:

1. The simulation results show that the dynamic pressure energy and static pressure energy of the electrolyte fluid can be effectively adjusted by changing the degree of convergence of the electrolyte outlet. Moreover, higher dynamic pressure energy can be obtained by sacrificing dynamic pressure energy, which may bring positive effects in terms of ECM performance.
2. The experimental results obtained with different degrees of convergence of the electrolyte outlet show that moderate energy conversion of electrolyte fluid can achieve better surface quality and MRR. However, excessive sacrifice of fluid dynamic pressure energy will also worsen ECM performance.
3. The experimental results obtained under constant-current conditions show that the voltage increment in the convergent flow mode is smaller than that in the normal outlet mode. This may be because in the convergent flow mode, the static pressure of the electrolyte can effectively compress the gas product volume and reduce the resistivity of the machining gap.
4. Comprehensive simulation and experimental results indicate that the moderate energy conversion of electrolyte fluid can not only achieve better machining performance but also improve the utilization efficiency of electrical energy in the ECM process.

Author Contributions: Methodology, Y.Z.; Formal analysis, W.C.; Data curation, M.C.; Writing—original draft, Z.G. All authors have read and agreed to the published version of the manuscript.

Funding: This research was funded by the Jiangsu Agricultural Science and Technology Innovation Fund (CX(21)3154) and the National Natural Science Foundation of China (52175438).

Institutional Review Board Statement: Not applicable.

Informed Consent Statement: Not applicable.

Data Availability Statement: Data are contained within the article.

Conflicts of Interest: The authors declare no conflict of interest.

References

1. Rajurkar, K.P.; Zhu, D.; McGeough, J.A.; Kozak, J.; De Silva, A. New developments in electro-chemical machining. *CIRP Ann. Manuf. Technol.* **1999**, *48*, 567–579. [CrossRef]
2. Geethapriyan, T.; Muthuramalingam, T.; Palani, I.A.; Mani, J.; Nikolaos, E.K.; Emmanouil, L.P.; Panagiotis, K.O. Influence of Silver-Coated Tool Electrode on Electrochemical Micromachining of Incoloy 825. *Coatings* **2023**, *13*, 963. [CrossRef]
3. Xu, Z.Y.; Wang, Y.D. Electrochemical machining of complex components of aero-engines: Developments, trends, and technological advances. *Chin. J. Aeronaut.* **2019**, *34*, 28–53. [CrossRef]
4. Sharma, V.; Patel, D.S.; Jain, V.K.; Ramkumar, J. Wire electrochemical micromachining: An overview. *Int. J. Mach. Tools Manuf.* **2020**, *155*, 103579. [CrossRef]
5. Zhan, S.D.; Liu, Z.Z.; Dong, B.Y.; Liu, W.D.; Zhao, Y.H. Cathodic discharge plasma in electrochemical jet machining: Phenomena, mechanism and characteristics. *Int. J. Mach. Tools Manuf.* **2023**, *187*, 104015. [CrossRef]
6. Klocke, F.; Zeis, M.; Klink, A.; Veselovac, D. Experimental research on the electrochemical machining of modern titanium- and nickel-based alloys for aero engine components. *Procedia CIRP* **2013**, *6*, 368. [CrossRef]
7. Chen, Y.L.; Zhou, X.C.; Chen, P.X.; Wang, Z.Q. Electrochemical machining gap prediction with multi-physics coupling model based on two-phase turbulence flow. *Chin. J. Aeronaut.* **2020**, *33*, 1057–1063. [CrossRef]
8. Lin, J.; Zhu, D.; Hu, X. Flow field design and experimental investigation of the electrochemical trepanning of a diffuser with a liquid-increasing seam. *Int. J. Adv. Manuf. Technol.* **2021**, *112*, 2533–2545. [CrossRef]
9. Liang, H.; Yan, C.; Zhang, X.Y.; Zhang, J.H.; Lei, Y.; Li, Y.; Fan, Q.M. Research on the multi-physics field coupling simulation of aero-rotor blade electrochemical machining. *Sci. Rep.* **2021**, *11*, 2817.
10. Ge, Y.C.; Zhu, Z.W.; Ma, Z.; Wang, D.Y. Large allowance electrochemical turning of revolving parts using a universal cylindrical electrode. *J. Mater. Process. Technol.* **2018**, *258*, 89–96. [CrossRef]
11. Xu, Z.Y.; Sun, L.Y.; Hu, Y.; Zhang, J.C. Flow field design and experimental investigation of electrochemical machining on blisk cascade passage. *Int. J. Adv. Manuf. Technol.* **2014**, *71*, 459–469. [CrossRef]
12. Zhu, D.; Zhu, D.; Xu, Z.Y.; Xu, Q.; Liu, J. Investigation on the flow field of W-shape electrolyte flow mode in electrochemical machining. *J. Appl. Electrochem.* **2010**, *40*, 525–532. [CrossRef]
13. Gu, Z.Z.; Zhu, D.; Xue, T.Y.; Liu, A.; Zhu, D. Investigation on flow field in electrochemical trepanning of aero engine diffuser. *Int. J. Adv. Manuf. Technol.* **2017**, *89*, 877–884. [CrossRef]
14. Zhu, D.; Gu, Z.Z.; Xue, T.Y.; Zhu, D. Flow Field Design in Electrochemical Machining of Diffuser. *Procedia CIRP* **2016**, *42*, 121–124. [CrossRef]
15. Wang, Y.D.; Xu, Z.Y.; Liu, J.; Zhang, A.; Xu, Z.L.; Meng, D.M.; Zhao, J.B. Study on flow field of electrochemical machining for large size blade. *Int. J. Mech. Sci.* **2021**, *190*, 106018. [CrossRef]
16. Li, H.S.; Wang, G.Q.; Qu, N.S.; Zhu, D. Through-mask electrochemical machining of a large-area hole array in a serpentine flow channel. *Int. J. Mach. Tools Manuf.* **2016**, *89*, 933–940. [CrossRef]
17. Liu, Y.; Liu, J.; Zhu, D. Flow field optimization of pulse dynamic electrochemical machining for serpentine channels on stainless steel plates. *Int. J. Adv. Manuf. Technol.* **2023**, *129*, 3563–3576. [CrossRef]
18. Tang, L.; Yang, F.; Gan, W.M. Electrochemical machining flow field simulation and experimental verification for irregular vortex paths of a closed integer impeller. *Int. J. Adv. Manuf. Technol.* **2016**, *83*, 275–283. [CrossRef]
19. Liu, Y.; Qu, N.S. Improvements to machining surface quality by controlling the flow direction of electrolyte during electrochemical sinking and milling of titanium alloy. *Sci. China Technol. Sci.* **2020**, *63*, 2698–2708. [CrossRef]
20. Yang, F.; Zhang, J.; Zhao, S.; Guo, C.A. Analysis of flow field for electrochemical machining deep spiral hole with gradually changing groove section. *Int. J. Adv. Manuf. Technol.* **2020**, *107*, 3267–3275. [CrossRef]
21. Ge, Y.C.; Zhu, Z.W.; Ma, Z.; Wang, D.Y. Tool Design and Experimental Study on Electrochemical Turning of Nickel-Based Cast Superalloy. *J. Electrochem. Soc.* **2018**, *165*, E162–E170. [CrossRef]
22. Zou, X.H.; Fang, X.L.; Zeng, Y.B.; Zhu, D. A high efficiency approach for wire electrochemical micromachining using cutting edge tools. *Int. J. Adv. Manuf. Technol.* **2017**, *91*, 3943–3952.
23. Jia, J.L.; Hao, Y.J.; Ma, B.J.; Xu, T.C.; Li, S.C.; Xu, J.; Zhong, L. Gas–liquid two-phase flow field analysis of two processing teeth spiral incremental cathode for the deep special-shaped hole in ECM. *Int. J. Adv. Manuf. Technol.* **2023**, *127*, 5831–5846. [CrossRef]
24. Tang, L.; Ma, Y.C.; Xue, R.R.; Bo, Y.F.; Zhang, J.J.; Zhang, j. Optimization and experimental study on cathode structure of electrochemical machining titanium alloy inner helix. *Int. J. Adv. Manuf. Technol.* **2024**, *130*, 1141–1149. [CrossRef]
25. Chai, M.X.; Li, Z.Y.; Yan, H.J.; Huang, Z.X. Flow field characteristics analysis of interelectrode gap in electrochemical machining of film cooling holes. *Int. J. Adv. Manuf. Technol.* **2021**, *112*, 525–536. [CrossRef]
26. Shin, H.S.; Kin, B.H.; Chu, C.N. Analysis of the side gap resulting from micro electrochemical machining with a tungsten wire and ultrashort voltage pulses. *J. Micromechanics Microengineering* **2008**, *18*, 75009. [CrossRef]
27. Fang, X.L.; Qu, N.S.; Zhang, Y.D.; Xu, Z.Y.; Zhu, D. Effects of pulsating electrolyte flow in electrochemical machining. *J. Mater. Process. Technol.* **2014**, *214*, 36–43. [CrossRef]
28. Qu, N.S.; Hu, Y.; Zhu, D.; Xu, Z.Y. Electrochemical machining of blisk channels with progressive-pressure electrolyte flow. *Mater. Manuf. Process.* **2014**, *29*, 572–578. [CrossRef]
29. Hu, X.Y.; Zhu, D.; Li, J.B.; Gu, Z.Z. Flow field research on electrochemical machining with gas film insulation. *J. Mater. Process. Technol.* **2019**, *267*, 247–256. [CrossRef]

30. Hewidy, M.S.; Ebeid, S.J.; Rajurkar, K.P.; El-Safti, M.F. Electrochemical machining under orbital motion conditions. *J. Mater. Process. Technol.* **2001**, *109*, 339–346. [CrossRef]
31. Zhao, R.C.; Huang, L.; Zhao, H.Y.; Cao, Y.; Tian, W.J.; Wang, N. Study of Mask Electrochemical Machining for Ring Narrow Groove under the Action of Multiple Physical Fields. *Coatings* **2022**, *12*, 605. [CrossRef]
32. Cao, W.J.; Wang, D.Y.; Guo, H.T.; Zhu, D. Improvement on profile accuracy of convex structure during counter-rotating electrochemical machining by periodically changing electrolyte flow direction. *J. Manuf. Process.* **2023**, *102*, 79–94. [CrossRef]
33. Xu, J.W.; Zhu, D.; Lin, J.H.; Hu, X.Y. Flow field design and experimental investigation of electrochemical trepanning of diffuser with a special structure. *Int. J. Adv. Manuf. Technol.* **2020**, *107*, 1551–1558. [CrossRef]
34. Ge, Z.H.; Chen, W.W.; Zhu, Y.W. Simulation and Experimental Study on Improving Electrochemical Machining Stability of Highly Convex Structures on Casing Surfaces Using Backwater Pressure. *Chin. J. Mech. Eng.* **2021**, *35*, 98. [CrossRef]
35. Wang, G.Q.; Jiang, S.; Ni, S.D.; Zhang, Y. Study of Mass Transfer Enhancement of Electrolyte Flow Field by Rotating Cathode in Through-Mask Electrochemical Micromachining. *Micromachines* **2023**, *14*, 1398. [CrossRef] [PubMed]
36. Wang, Y.D.; Xu, Z.Y.; Meng, D.; Liu, L.; Fang, Z.D. Multi-Physical Field Coupling Simulation and Experiments with Pulse Electrochemical Machining of Large Size TiAl Intermetallic Blade. *Metals* **2023**, *13*, 985. [CrossRef]
37. Subbaiah, T.; Vijetha, P.; Marandi, B.; Sanjay, K.; Manickam, M. Ionic Mass Transfer at Point Electrodes Located at Cathode Support Plate in an Electrorefining Cell in Presence of Rectangular Turbulent Promoters. *Sustainability* **2022**, *14*, 880. [CrossRef]
38. Sarangi, C.K.; Sheik, A.R.; Marandi, B.; Ponnam, V.; Ghoshet, M.K.; Sanjay, K.; Minakshi, M.; Subbaiah, T. Recovery of Tellurium from Waste Anode Slime Containing High Copper and High Tellurium of Copper Refineries. *Sustainability* **2023**, *15*, 11919. [CrossRef]

Disclaimer/Publisher's Note: The statements, opinions and data contained in all publications are solely those of the individual author(s) and contributor(s) and not of MDPI and/or the editor(s). MDPI and/or the editor(s) disclaim responsibility for any injury to people or property resulting from any ideas, methods, instructions or products referred to in the content.